

Clarifying Self Seed in 391-nm N_2^+ Air Lasing by Vectorially Structured Light Fields

Jingsong Gao,^{1,2} Yang Wang,¹ Chengyin Wu,¹ Hongbing Jiang,^{1,*} Yunquan Liu,^{1,†} and Meng Han^{2,‡}

¹*State Key Laboratory for Mesoscopic Physics and Collaborative Innovation Center of Quantum Matter, School of Physics, Peking University, Beijing 100871, China*

²*James R. Macdonald Laboratory, Department of Physics, Kansas State University, Manhattan, Kansas, 66506, USA*

(Dated: February 4, 2025)

A single intense near-infrared femtosecond laser beam can generate ultraviolet N_2^+ lasing at 391 nm in the air, offering a promising tool for remote sensing. One of the key debates regarding its mechanism is whether it is seeded by a self-generated spectral component, such as the second harmonic, which is inevitably produced by the charge gradient in the laser plasma filament. In this study, we generated both radially and azimuthally polarized N_2^+ lasing at 391 nm, in contrast to that the second harmonic in argon is found near zero at the azimuthal polarization case. By characterizing the spatial phase distribution of the radially polarized 391-nm lasing, we concluded that the phase of the 391-nm lasing aligns with the driving field, thereby ruling out the hypothesis of self-seeding by the second harmonic. Our work also provides a promising method to remotely generate vectorially structured ultraviolet light fields.

Air lasing is a phenomenon in which laser-induced air produces cavity-free coherent light [1–3], effectively acting as a laser. Unlike conventional lasers, which require a physical gain medium (such as a crystal, gas, or liquid) within a cavity to amplify light, air lasing occurs in the atmosphere without the need for a physical cavity. Among various types of air radiations, N_2^+ air lasing [4], particularly the 391-nm radiation corresponding to the transition between ground vibrational states from B to X ionic states, is one of the most debated phenomena. It has garnered significant interest due to its contradiction with well-established strong-field theories [5–21] and its promising applications [22–24]. Previous experiments [25, 26] have clearly demonstrated that 391-nm lasing can be effectively amplified by an external seed. However, a fundamental question remains unresolved: is the 391-nm lasing process seeded by self-generated spectral components, such as self-phase modulation (SPM) or second harmonic generation (SHG)?

The prevailing use of Ti:sapphire (Ti:Sa) laser pulses complicates this question further, as the wavelength of the driving field is around 800 nm, with its second harmonic overlapping with the 391-nm transition. If the 391-nm lasing is self-seeded, it can be attributed to superfluorescence or light amplification by stimulated emission of radiation (i.e., laser action). Conversely, if the 391-nm lasing process does not involve any seeding, it is strictly amplified spontaneous emission (ASE) [1]. For few-cycle Ti:Sa pulses, the spectrum typically spans from 550 nm to 1000 nm, and the SPM during the focusing process can easily generate a supercontinuum extending down to 391 nm, especially at high pressure [5, 10], serving as a seed. However, for the more commonly used multi-cycle Ti:Sa pulses with durations of 30–50 fs, SPM cannot broaden the spectrum to 391 nm in the low pressure below one atmosphere, ruling out SPM as a self-seeding mechanism. Thus, the prevailing viewpoint [27, 28] is that 391-nm

lasing is seeded by the second harmonic generated by the charge gradient in the laser plasma filament [29]. Therefore, investigating the potential self-seeding mechanisms in 391-nm lasing remains an important and unresolved question.

Structured light with a customized profile in space and time can now be well constructed, due to the development of laser tailoring techniques [30–33]. One dramatic paradigm is cylindrical vector beams that possess cylindrical symmetric polarization in space [34], as shown in Fig. 1(a). A laser plasma filament also exhibits cylindrical symmetry along the light propagation direction, resulting in a charge gradient along the radial direction in the beam cross plane, similar to the radially polarized beam and orthogonal to the azimuthally polarized beam. Therefore, the key idea of our method is to employ these vectorial features in the laser-plasma interaction to clarify the role of the SHG in the 391-nm N_2^+ lasing.

Here we drive the 391-nm lasing in N_2 and the second harmonic in argon with cylindrical vector beams. We generate both radially and azimuthally polarized 391-nm N_2^+ lasing with equal intensities, whereas the second harmonic disappears when switching from radial to azimuthal polarization. By analyzing the focal properties of the cylindrical vector beam, we show that the spatial phase of the N_2^+ lasing is synchronized with the spatial phase of the pump light rather than being double that of the pump light. We demonstrate that the phase distribution of the driving field is directly transferred to the generated 391-nm lasing. By combining the results of 391-nm N_2^+ lasing and the second harmonic generation in argon, we conclude that 391-nm N_2^+ lasing driven by a multi-cycle Ti:sa laser pulse does not involve any self-seeding mechanism and is therefore consistent with ASE.

The experimental setup is depicted in Fig. 1(a). The s-polarized Gaussian laser pulses are launched from a Ti:Sa regen amplifier (Spectra-Physics Spitfire Ace) with a cen-

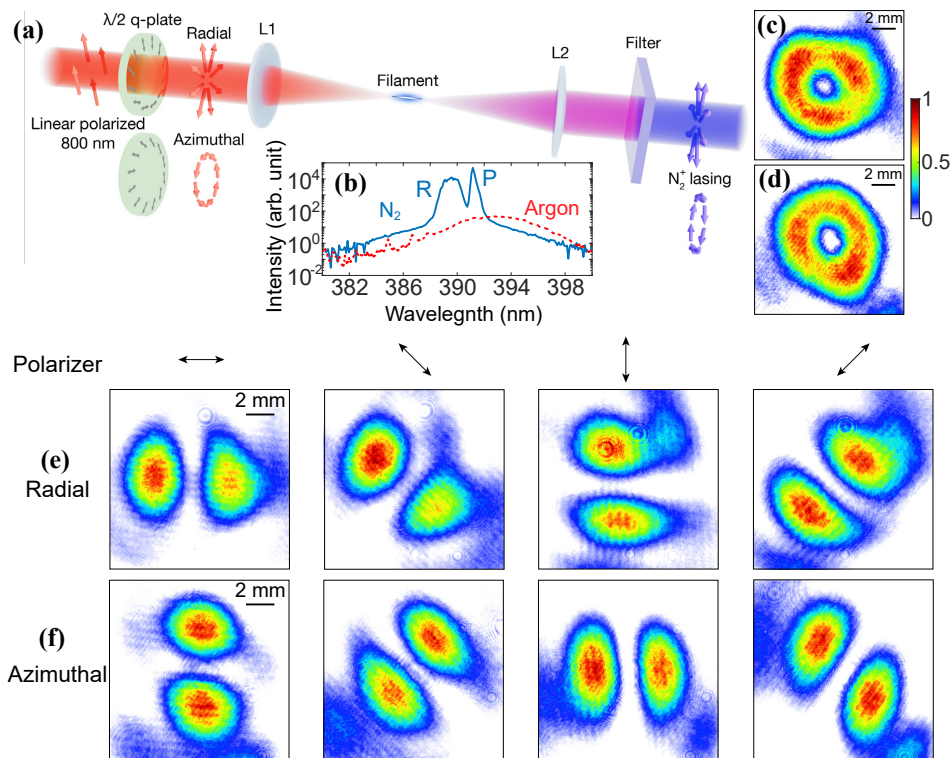


FIG. 1. (a) Schematic of generation of vectorial N_2^+ air laser. (b) Measured 391-nm N_2^+ laser spectrum (blue solid line) and the second harmonic spectrum from argon (red dashed line). (c, d) Measured beam profiles of the generated radially (c) and azimuthally (d) polarized 391-nm laser. (e) Measured radially polarized 391-nm laser beam profiles after passing a polarizer oriented along different angles marked with black arrows. (f) Corresponding experimental results for azimuthally polarized 391-nm laser.

tral wavelength of 790 nm, a pulse duration of 35 fs, a repetition of 1 kHz, and a single pulse energy of 3 mJ. After passing through a thin half-wave q-plate [35, 36], the 790 nm Gaussian beam becomes a cylindrical vector beam with spatial variant polarization. Then, the cylindrical vector beam is focused on the 10-mbar pure nitrogen gas by a lens with a focal length of 30 cm. The N_2^+ laser is emitted from the laser-induced plasma and filtered by a band-pass filter with a central wavelength of 390 and a bandwidth of 10 nm. After the filter, we recorded the beam profile by a charge-coupled device (CCD) and detected the spectrum by a fiber head connected to a grating spectrometer. The angle of the q-plate is set to make the pump beam radially and azimuthally polarized, respectively, where the fast axis orientation of the q-plate and the spatial polarization distribution of the pump beam are depicted in Fig. 1(a).

Figure 1(b) compares the measured spectra of the 391-nm N_2^+ laser and the SHG from argon. For the 391-nm laser, it displays two peaks corresponding to the P and R branches of rotational transitions. The contribution from SPM can be ruled out from the weak and symmetrical pedestals on the two sides of the 391-nm laser peak. If it is seeded by SPM, the pedestal will show some intensity

above the noise level at the wavelength larger than 391 nm [5].

Figures 1(c) and 1(d) depict the beam intensity profiles of the generated radially and azimuthally polarized 391-nm laser, respectively. Both profiles exhibit a donut-shaped distribution, indicating the presence of a polarization singularity at the beam center. To examine the spatial distribution of the polarization state within the beam plane, we present the beam intensity profiles in Figs. 1(e) and 1(f) after passing through a polarizer, with the polarizer's orientation indicated above each figure. Additional polarization analyses, obtained by rotating the polarizer orientation at various positions within the beam profile, are provided in the Supplemental Material (SM). The polarizations at all positions are linear, possessing radial polarization and azimuthal polarization characteristics, respectively. These results confirm that the generated radially and azimuthally polarized 391-nm laser exhibit approximately equal intensities. Furthermore, the polarization distribution of the 391-nm laser mirrors that of the driving field in both radial and azimuthal configurations.

The SHG can occur in an isotropic gaseous medium if the plasma within the irradiated volume is inhomogeneous.

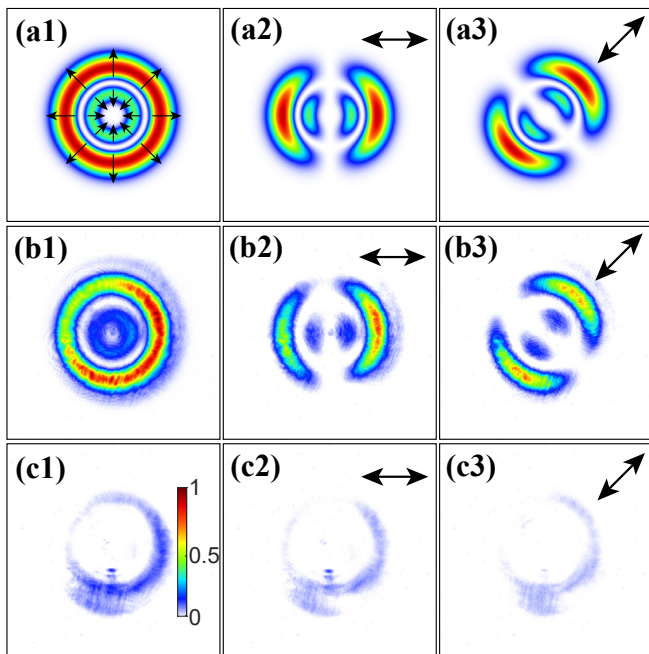


FIG. 2. Generation and polarization characterization of the second harmonic in argon driven by vectorial light fields. The first column shows the beam profile of the second harmonic. The second and third columns show the beam profile after passing a polarizer with the orientation marked in the upper-right corner. **(a1-a3)** Calculated beam intensity profile driven by radially polarized light fields. The arrows in (a1) indicate the polarization state locally. **(b1-b3)** Corresponding experimental results driven by radially polarized light fields. **(c1-c3)** Corresponding experimental results driven by azimuthally polarized light fields, whereas the theoretical results are zero. Note that the intensities in (c1-c3) are normalized to those in (b1-b3).

geneous. The resulting ponderomotive force acts outward from the center of the pump beam, creating an uneven electron distribution. This redistribution pushes electrons away from the center of the focused beam, ultimately leading to the SHG. The second order polarization can be written as [29, 37],

$$\vec{P}(2\omega) \propto [1/2\nabla E_P^2 + \frac{2(\vec{E}_P \cdot \nabla \ln n_e)\vec{E}_P}{\epsilon_p}], \quad (1)$$

where \vec{E}_P is the driving electric field in the focal plane, ϵ_p is the plasma dielectric constant, and n_e is the plasma density. In the nonuniform plasma, the last term in Eq.(1) dominates the SHG. $\nabla \ln n_e$ stands for the electron gradient along the radial direction. Therefore, the product between the driving field and the electron gradient, $\vec{E}_P \cdot \nabla \ln n_e$, will be zero for the azimuthally polarized driving field and be a maximum for the radially polarized driving field.

In order to eliminate the influence of air lasing and observe the beam profile of a pure SHG signal, we use argon as the target gas, where there is no significant atomic

emission lines around 400 nm. The measured SH spectrum is shown in Figure 1(b). In Figure 2, we illustrate the theoretical and experimental results of the SH in argon. Figure 2(a1) shows the calculated SH beam profile intensity with the arrows indicating the polarization state locally, driven by the radially polarized light field, based on Eq. (1). Figures 2(a2) and (a3) show the beam profile after passing a polarizer oriented along horizontal and 45° directions. See SM for the simulation details. The theoretical result shows there are two concentric rings in the beam profile with a phase difference of π . In contrast, in the azimuthal driving field, the electron gradient is perpendicular to the driving electric field, and thus the SH intensity is near zero. Figures 2(b1-b3) and 2(c1-c3) show our measurement results driven by radially and azimuthally polarized light fields, respectively. The result in the radial case indeed shows two rings in the beam profile. The measured SH intensity by azimuthally polarized fields is near zero, agreeing well with our simulation on Eq. (1).

The absence of SHG in the azimuthal case indicates that SH plays a minimal role in the 391-nm lasing, as we generated azimuthally polarized 391-nm lasing with approximately equal intensities. This is reasonable and consistent with the theoretical expectation because the effective gain region is located near the peak of the driving field's intensity, where the gradient of the plasma is almost zero, i.e., there is no SHG. As a result, in the laser filamentation, the SH and the gain region are inherently not overlapped in space.

Figure 3 provides further experimental evidence from the perspective of spatial phase. The key feature of the seeded air lasing is that the amplified light retains the phase of the seed [20, 21], which can be a criteria for checking the 391-nm lasing driven by a single laser beam. In Figure 3, we used a cylindrical lens to examine the spatial phase distribution in the beam profile. If the 391-nm lasing is phase-synchronized with the driving field, as depicted in Fig. 3(a), the two lobes after passing through a polarizer should exhibit opposite phases. Consequently, using a cylindrical lens, the two lobes cannot be focused together, and the resulting intensity pattern in the focal plane would still show two distinct stripes, as shown in Fig. 3(c). Conversely, if the 391-nm lasing is seeded by SH, the spatial phase would double. In this scenario, shown in Fig. 3(b), the two lobes after passing through a polarizer would have the same phase, allowing them to focus onto a single strip, as shown in Fig. 3(d). This would produce a dominant beam in the focal plane. Figure 3(e) illustrates our experimental results, which align with the calculated case for phase synchronization, confirming the phase relationship of the 391-nm lasing with the driving field. It should be mentioned that we only illustrate the case of the y component of the radially polarized case here. Indeed, the measured phase difference of the two lobes in each panel of Figures (e-f) is π . In

SM, we present simulation details for the calculation of the beam focusing with the modified Richard-Wolf vectorial diffraction method for a cylindrical lens.

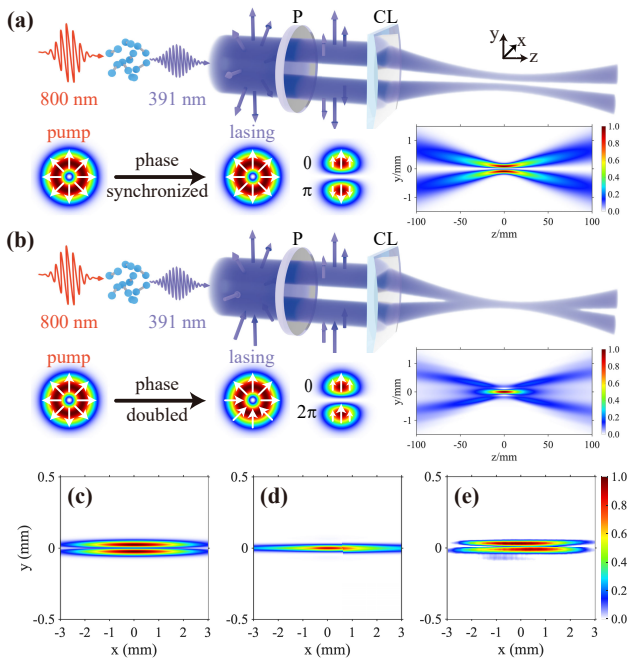


FIG. 3. Phase distribution measurement of the radially polarized 391-nm N_2^+ lasing by cylindrical lens. (a) Calculated results when the spatial phase of 391-nm lasing is synchronized with the driving field. (b) Calculated results when the spatial phase of 391-nm lasing is double that of the driving field. (c, d) Calculated beam profiles in the focus plane in the scenarios of (a) and (b), respectively. (e) Experimental result.

In conclusion, our study provides critical insights into the generation mechanism of N_2^+ lasing at 391 nm, specifically addressing the debated role of self-seeding by the second harmonic. By successfully generating both radially and azimuthally polarized 391-nm lasing and analyzing the spatial phase distribution, we demonstrated that the lasing phase is synchronized with the driving field, effectively ruling out second harmonic self-seeding. Our experimental results suggest the 391-nm lasing originates from the ASE process. This work not only resolves a key aspect of the lasing mechanism but also introduces a method for remotely generating ultraviolet vectorially structured light fields, offering new possibilities for applications in advanced remote sensing and laser physics.

Kansas State group was supported by the Chemical Sciences, Geosciences and Biosciences Division, Office of Basic Energy Sciences, Office of Science, US Department of Energy, grant no. DE-FG02-86ER13491. The authors thank Jiahao Dong from University of Shanghai for Science and Technology for his assistance in figure design.

* hbjiang@pku.edu.cn

† yunquan.liu@pku.edu.cn

‡ meng9@ksu.edu

- [1] Q. Luo, W.-w. Liu, and S. Chin, Lasing action in air induced by ultra-fast laser filamentation, *Applied physics B* **76**, 337 (2003).
- [2] P. R. Hemmer, R. B. Miles, P. Polynkin, T. Siebert, A. V. Sokolov, P. Sprangle, and M. O. Scully, Stand-off spectroscopy via remote generation of a backward-propagating laser beam, *Proceedings of the National Academy of Sciences* **108**, 3130 (2011).
- [3] A. Dogariu, J. B. Michael, M. O. Scully, and R. B. Miles, High-gain backward lasing in air, *Science* **331**, 442 (2011).
- [4] J. Yao, B. Zeng, H. Xu, G. Li, W. Chu, J. Ni, H. Zhang, S. L. Chin, Y. Cheng, and Z. Xu, High-brightness switchable multiwavelength remote laser in air, *Physical Review A—Atomic, Molecular, and Optical Physics* **84**, 051802 (2011).
- [5] H. Xu, E. Lötstedt, A. Iwasaki, and K. Yamanouchi, Sub-10-fs population inversion in $n2+$ in air lasing through multiple state coupling, *Nature communications* **6**, 8347 (2015).
- [6] Y. Liu, P. Ding, G. Lambert, A. Houard, V. Tikhonchuk, and A. Mysyrowicz, Recollision-induced superradiance of ionized nitrogen molecules, *Physical Review Letters* **115**, 133203 (2015).
- [7] Q. Zhang, H. Xie, G. Li, X. Wang, H. Lei, J. Zhao, Z. Chen, J. Yao, Y. Cheng, and Z. Zhao, Sub-cycle coherent control of ionic dynamics via transient ionization injection, *Communications Physics* **3**, 50 (2020).
- [8] J. Yao, S. Jiang, W. Chu, B. Zeng, C. Wu, R. Lu, Z. Li, H. Xie, G. Li, C. Yu, et al., Population redistribution among multiple electronic states of molecular nitrogen ions in strong laser fields, *Physical review letters* **116**, 143007 (2016).
- [9] M. Britton, P. Laferriere, D. H. Ko, Z. Li, F. Kong, G. Brown, A. Naumov, C. Zhang, L. Arissian, and P. Corkum, Testing the role of recollision in $n 2+$ air lasing, *Physical review letters* **120**, 133208 (2018).
- [10] T. Ando, E. Lötstedt, A. Iwasaki, H. Li, Y. Fu, S. Wang, H. Xu, and K. Yamanouchi, Rotational, vibrational, and electronic modulations in $n 2+$ lasing at 391 nm: Evidence of coherent $b \sigma 2 u+-x \sigma 2 g+-a \pi 2 u$ coupling, *Physical Review Letters* **123**, 203201 (2019).
- [11] X. Zhang, Q. Lu, Z. Zhang, Z. Fan, D. Zhou, Q. Liang, L. Yuan, S. Zhuang, K. Dorfman, and Y. Liu, Coherent control of the multiple wavelength lasing of $n \frac{+}{2}$: coherence transfer and beyond, *Optica* **8**, 668 (2021).
- [12] Y. Chen, H. Lei, Q. Wang, H. Xie, H. Zhang, X. Lu, N. Zhang, S. Huang, Y. Wu, J. Liu, et al., Multiphoton resonance meets tunneling ionization: High-efficient photoexcitation in strong-field-dressed ions, *Physical Review Letters* **133**, 113201 (2024).
- [13] C. Yuen and C. Lin, Probing vibronic coherence in charge migration in molecules using strong-field sequential double ionization, *Physical Review A* **109**, L011101 (2024).
- [14] C.-H. Yuen and C.-D. Lin, Coherence from multiorbital tunneling ionization of molecules, *Physical Review A* **108**, 023123 (2023).
- [15] M. Richter, M. Lytova, F. Morales, S. Haessler,

- O. Smirnova, M. Spanner, and M. Ivanov, Rotational quantum beat lasing without inversion, *Optica* **7**, 586 (2020).
- [16] J. Gao, X. Zhang, Y. Wang, J. Dong, M. Lei, Y. Liu, C. Wu, Q. Gong, and H. Jiang, Controlling the polarization of nitrogen ion lasing, *The Journal of Physical Chemistry Letters* **15**, 3805 (2024).
- [17] H. Xie, H. Lei, G. Li, Q. Zhang, X. Wang, J. Zhao, Z. Chen, J. Yao, Y. Cheng, and Z. Zhao, Role of rotational coherence in femtosecond-pulse-driven nitrogen ion lasing, *Physical Review Research* **2**, 023329 (2020).
- [18] J. Gao, X. Zhang, Y. Wang, Y. Fang, Q. Lu, Z. Li, Y. Liu, C. Wu, Q. Gong, Y. Liu, *et al.*, Structured air lasing of $n=2+$, *Communications Physics* **6**, 97 (2023).
- [19] C. Kleine, M.-O. Winghart, Z.-Y. Zhang, M. Richter, M. Ekimova, S. Eckert, M. J. Vrakking, E. T. Nibbering, A. Rouzée, and E. R. Grant, Electronic state population dynamics upon ultrafast strong field ionization and fragmentation of molecular nitrogen, *Physical Review Letters* **129**, 123002 (2022).
- [20] H. Mei, J. Gao, K. Wang, J. Dong, Q. Gong, C. Wu, Y. Liu, H. Jiang, and Y. Liu, Amplification of light pulses with orbital angular momentum (oam) in nitrogen ions lasing, *Optics Express* **31**, 31912 (2023).
- [21] B. Shen, P. Xue, X. Lu, J. Wang, N. Zhang, S. Huang, Y. Chen, P. Qi, L. Lin, J. Yao, *et al.*, High-gain, high-order vortex air lasing generated by plasma amplification, *Laser & Photonics Reviews* , 2401276 (2024).
- [22] Z. Liu, J. Yao, H. Zhang, B. Xu, J. Chen, F. Zhang, Z. Zhang, Y. Wan, W. Chu, Z. Wang, *et al.*, Extremely nonlinear raman interaction of an ultrashort nitrogen ion laser with an impulsively excited molecular wave packet, *Physical Review A* **101**, 043404 (2020).
- [23] N. Zhang, H. Xie, H. Zhang, X. Lu, Y. Chen, Y. Wu, Y. Cheng, and J. Yao, Electronic-resonance-enhanced coherent raman spectroscopy with a single femtosecond laser beam, *Laser & Photonics Reviews* **17**, 2300020 (2023).
- [24] H. Lei, J. Yao, J. Zhao, H. Xie, F. Zhang, H. Zhang, N. Zhang, G. Li, Q. Zhang, X. Wang, *et al.*, Ultraviolet supercontinuum generation driven by ionic coherence in a strong laser field, *Nature Communications* **13**, 4080 (2022).
- [25] J. Ni, W. Chu, C. Jing, H. Zhang, B. Zeng, J. Yao, G. Li, H. Xie, C. Zhang, H. Xu, *et al.*, Identification of the physical mechanism of generation of coherent $n=2+$ emissions in air by femtosecond laser excitation, *Optics express* **21**, 8746 (2013).
- [26] B. Xu, S. Jiang, J. Yao, J. Chen, Z. Liu, W. Chu, Y. Wan, F. Zhang, L. Qiao, R. Lu, *et al.*, Free-space $n=2+$ lasers generated in strong laser fields: the role of molecular vibration, *Optics Express* **26**, 13331 (2018).
- [27] Y. Liu, Y. Brelet, G. Point, A. Houard, and A. Mysyrowicz, Self-seeded lasing in ionized air pumped by 800 nm femtosecond laser pulses, *Optics express* **21**, 22791 (2013).
- [28] Y. Hu, Z. Ye, H. Li, C. Lu, F. Chen, J. Wang, S. Pan, M. Zhang, J. Gao, and J. Wu, Generation of vortex $n=2+$ lasing, *Optica* **10**, 682 (2023).
- [29] M. Beresna, P. G. Kazansky, Y. Svirko, M. Barkauskas, and R. Danielius, High average power second harmonic generation in air, *Applied Physics Letters* **95** (2009).
- [30] H. Rubinsztein-Dunlop, A. Forbes, M. V. Berry, M. R. Dennis, D. L. Andrews, M. Mansuripur, C. Denz, C. Alpmann, P. Banzer, T. Bauer, *et al.*, Roadmap on structured light, *Journal of Optics* **19**, 013001 (2016).
- [31] A. Forbes, M. De Oliveira, and M. R. Dennis, Structured light, *Nature Photonics* **15**, 253 (2021).
- [32] I. Cristiani, C. Lacava, G. Rademacher, B. J. Puttnam, R. S. Luis, C. Antonelli, A. Mecozzi, M. Shtaif, D. Cozzolino, D. Bacco, *et al.*, Roadmap on multimode photonics, *Journal of Optics* **24**, 083001 (2022).
- [33] Y. Shen, Q. Zhan, L. G. Wright, D. N. Christodoulides, F. W. Wise, A. E. Willner, K.-h. Zou, Z. Zhao, M. A. Porras, A. Chong, *et al.*, Roadmap on spatiotemporal light fields, *Journal of Optics* **25**, 093001 (2023).
- [34] Q. Zhan, Cylindrical vector beams: from mathematical concepts to applications, *Advances in Optics and Photonics* **1**, 1 (2009).
- [35] R. Dorn, S. Quabis, and G. Leuchs, Sharper focus for a radially polarized light beam, *Physical review letters* **91**, 233901 (2003).
- [36] G. Machavariani, Y. Lumer, I. Moshe, A. Meir, and S. Jackel, Efficient extracavity generation of radially and azimuthally polarized beams, *Optics letters* **32**, 1468 (2007).
- [37] D. Bethune, Optical second-harmonic generation in atomic vapors with focused beams, *Physical Review A* **23**, 3139 (1981).